www.czasopisma.pan.pl PAN www.journals.pan.pl

ARCHIVES of FOUNDRY ENGINEERING

ISSN (2299-2944)
Volume 2020
Issue 2/2020

13 – 18

10.24425/afe.2020.131295

2/2

Published quarterly as the organ of the Foundry Commission of the Polish Academy of Sciences

Influence of Zr on AlSi9Cu1Mg Alloy Cast in Ceramic

M. Matejka *, M. Kuriš, D. Bolibruchova, R. Pastirčák
Department of Technological Engineering, University of Zilina,
Univerzitna 1, 010 26 Zilina, Slovak Republic
* Corresponding author. E-mail address: marek.matejka@fstroj.uniza.sk

Received 13.08.2019; accepted in revised form 04.11.2019

Abstract

The article focuses on the analysis of the effect of Zr on the properties of the aluminium alloy AlSi9Cu1Mg. The effect of Zr was evaluated depending on the change in mechanical properties and heat resistance during a gradual addition of Zr with an increase of 0.05 wt. % Zr. Half of the cast experimental samples from each variant were heat treated by precipitation hardening T6 (hereinafter HT). The measured values in both states indicate an improvement of the mechanical properties, especially in the experimental variants with a content of Zr ≥ 0.20 wt. %. In the evaluation of R_m, the most significant improvement occurred in the experimental variant with an addition of Zr 0.25 wt. % after HT and E in the experimental variant with addition of Zr 0.20 wt. % after HT. Thus, a difference was found from the results of the authors defining the positive effect of Zr, in particular at 0.15 wt. %. When evaluating the microstructure of the AlSi9Cu1Mg alloy after Zr alloying, Zr phases are already eliminated with the addition of Zr 0.10 wt. %. Especially at higher levels of Zr ≥ 0.20 wt. %, long needle phases with slightly cleaved morphology are visible in the metal matrix. It can be stated that a negative manifestation of Zr alloying is expressed by an increase in gassing of experimental alloys, especially in variants with a content of Zr ≥ 0.15 wt. %. Experimental samples were cast into ceramic moulds. The development of an experimental alloy AlSi9Cu1Mg alloyed with Zr would allow the production of a more sophisticated material applicable to thin-walled Al castings capable of operating at higher temperature loads.

Keywords: Solidification process, Heat treatment, AlSi9Cu1Mg, AlZr15, Ceramic moulds

1. Introduction

Al-Si alloys are experiencing a significant development in the foundry industry, especially in the production of high-precision castings. AlSi9Cu1Mg alloy is one of the important representatives. Due to its higher Si content, the AlSi9Cu1Mg alloy has excellent run-in, low contraction and low susceptibility to hot cracking. Due to the Mg and Cu content, an alloy is obtained which is cured by precipitation due to the precipitated Mg_2Si and Al_2Cu phases. AlSi9Cu1Mg is a hypoeutectic alloy designed for thin-walled castings, which can be subsequently welded and used at higher temperatures around 200 °C. For the needs of the automotive and aerospace industries, there is a constant need to improve the properties of the materials originally used. One way to improve the properties of AlSi9Cu1Mg is to alloy with elements such as Mo, Cr, Ce, Ni or Zr. The aim is to improve not only the mechanical properties but also the heat resistance of the alloys, thereby increasing the usability of Al castings for applications above 250 °C. As a result, Al castings with significant reliefs can be produced for higher thermal loads or castings of more complicated design. Significant representatives are castings of gearboxes or engine blocks. Here the emphasis is on the lowest casting weight possible and the ability to work at high performances. The application of a more sophisticated alloy with improved mechanical properties and heat

resistance increases material savings by reducing engine block dimensions, improving the environmental aspect by reducing fuel consumption, and increasing performance by improving the resistance of Al castings to the operating thermal load generated during plant operation. The experimental part follows the work of the authors Vončina and Medved [1, 2], pointing to improvement of mechanical properties of curable alloys AlSi9Cu3 and AA2050 after alloying with Zr and Mo. The increase in mechanical properties in the experiment points to the effect of Zr release in the form of strengthening phases. Preferably, Zr is released in the form of Al_3Zr during the peritectic reaction, with a content of Zr ≥ 0.10 wt. %. The Al_3Zr phase is released in two significantly different crystallographic morphologies. The first one is the tetragonal system DO_{23} (Fig. 1a.) And the second is the coherent metastable system $L1_2$ (Fig. 1b.). [1-10]

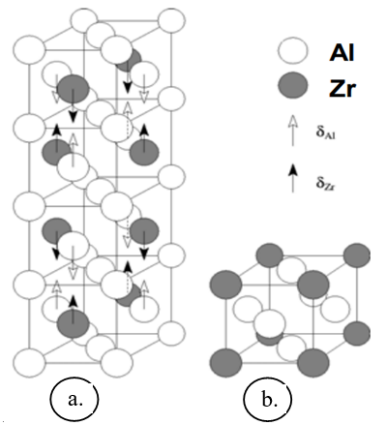

Fig. 1. Tetragonal system DO_{23} (a), coherent metastable system $L1_2$ (b) [7]

The effectiveness of Zr and its phases is closely related to the Mg, Cu content. These elements reduce the efficiency of Zr in Al alloys. Several works declare a visible elimination of Zr phases with an addition of Zr ≥ 0.08 wt. %. The positive effect on mechanical properties was also evident when Zr 0.15 wt. % was added. For contents Zr > 0.15 wt. %, several works by authors such as Vončina and Mahmudi [1, 4] mention that they do not observe an improvement in mechanical properties. Possibilities of the influence of alloys such as Zr on mechanical properties or thermal resistance of AlSi9Cu1Mg alloy, which is preferably used for production of thin-walled castings, point to the possibility of developing a more sophisticated alloy. Due to the development of similar material, especially for foundry technologies such as "investment casting", more complicated and operationally durable castings can be produced for the automotive and aerospace industries. [8-11]

2. Experimental part

The ceramic mould was prepared by a gradual process of dipping a wax tree in a ceramic slurry and then sprinkling it with a refractory grit. The ceramic mould consists of three basic layers ensuring the formation of a contact, insulating and solidifying coating. The material composition of each package is given in Table 1. Since STN EN 1706 norm does not define the minimum mechanical properties of the AlSi9Cu1Mg alloy for casting into ceramic moulds, sand casting values will be used to compare the results of the mechanical properties. These castings are characterized by similar heat dissipation i.e. similar crystallization.

Table 1.
Material composition of ceramics layers

Component	1. Layer	2. Layer	3. Layer
Binder	Primcotcote plus	SP-Ultra 2408	MatriXsol 30
Grain sand	Cerabed DS 60	Rancosil A	Molochite 30-80 DD
Component	**4. Layer**	**5. Layer**	
Binder	MatriXsol 30	MatriXsol 30	
Grain sand	Molochite 30-80 DD	Molochite 30-80 DD	

The ceramic mould (Fig. 2a.) with an approximate thickness of 3 mm, was annealed for min. 1.5 hours at 750 °C. Before the first contact with the molten alloy, the ceramic mould reached a temperature in the range of 510 to 540 °C. The samples were cast at a rate of 0.3 kg/s^{-1} from a casting height of 500 mm. The casting temperature was 750 ± 10 °C. After casting, the ceramic mould was cooled in air for 1 hour. The AlSi9Cu1Mg primary alloy was supplied by the manufacturer in a pre-vaccinated and pre-modified state.

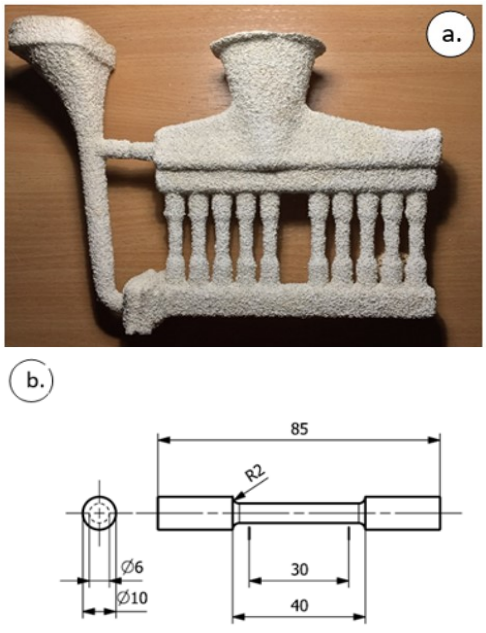

Fig. 2. Ceramic mould supplied by AluCAST (a), scheme of test sample (b)

The chemical composition of the primary alloy is shown in Table 2. The metallurgical process consisted of melting the primary alloy with the aim of producing the so-called reference alloy (without addition of Zr) and subsequent alloying with

AlZr15 master alloy. Zr was added in graduated amounts of 0.05 wt. % Zr (from 0.05 wt. % to 0.30 wt. % Zr). AlSi9Cu1Mg experimental alloys were not degassed throughout the experiment.

Table 2.
Chemical composition of primary alloy AlSi9Cu1Mg

Element	Si	Fe	Cu	Mn	Mg	Cr
wt. %	8.04	0.13	0.65	0.07	0.39	-
Element	Ni	Zn	Pb	Sn	Ti	
wt. %	-	0.004	-	0.01	0.18	

AlZr15 master alloy was associated with impaired melt solubility. The melt had to be preheated to a temperature of 770 ± 10 °C, thereby creating conditions to increase the gassing of hydrogen and the occurrence of possible defects. After casting of the experimental variants with the addition of Zr 0.00 wt. % to 0.30 wt. %, the HT process, brought about by precipitation hardening T6, followed. HT was performed on 5 from the total of 10 experimental samples (Fig. 2b.) from each experimental variant. The T6 heat treatment process is shown in Figure 3.

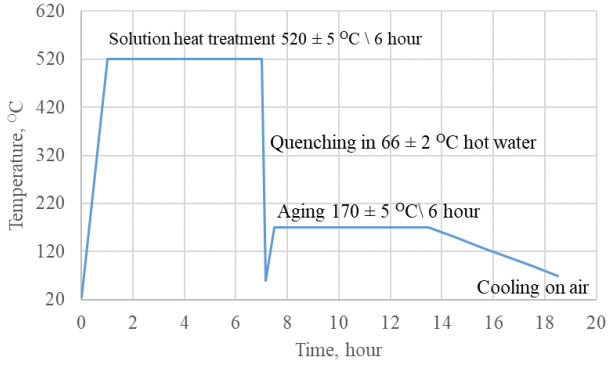

Fig. 3. Graphical show of heat treatment by precipitation hardening T6 of experimental samples alloys AlSi9Cu1Mg

2.1. Density Index and Thermal Analysis

The resulting mechanical properties of Al alloys are closely related to the melt solubility of hydrogen. Due to the absence of degassing of experimental alloys, it was possible to observe, with increasing Zr content in AlSi9Cu1Mg alloy, a sharp increase in density index (hereinafter DI). The test procedure consisted of casting two samples into 60 ml. test dies followed by solidification at atmospheric pressure and negative pressure ranging from 0.097 to 0.094 MPa for 4 min. The most significant increase of the DI index is observed for alloyed variants with content of Zr > 0.10 wt. % (Fig 4). The effect of the absence of melt degassing and the alloying process contributed to the increase in gassing in AlSi9Cu1Mg experimental alloys. The DI index increase is already observed in the experimental variant with an addition of Zr 0.05 wt. % where the DI index is 14.5 %. This represents an increase of 32.0 % over the reference variant, which reached a DI index of 11.0 %. A sharp increase occurs at a content Zr ≥ 0.15 wt. % to 0.25 wt. %, where the DI index ranges from 17.3 to 19.9 %. This represents a 57 and 80 % increase over the reference alloy. Given the content of Zr, large Zr phases are precipitated, as can be seen in Figure 9. in Chapter 2.2. When evaluating the macrostructures (Fig. 5) of the experimental samples with the addition of Zr 0.20 wt. % and 0.30 wt. % (Fig. 5b. and 5c.), hydrogen release was observed in the form of larger pores than in the reference samples (Fig. 5a.). It can be stated that the addition of Zr may cause an increase in hydrogen gasification in the AlSi9Cu1Mg alloy. The influence on the hydrogen bubble trapping can also be associated with the shape of the excluded Zr phases. These, at larger dimensions, can act as "scavengers" of the excreted hydrogen bubbles. The Zr phases are eliminated in needle morphology as early as at 630 °C, where the germs formed could trap the excreted hydrogen bubbles.

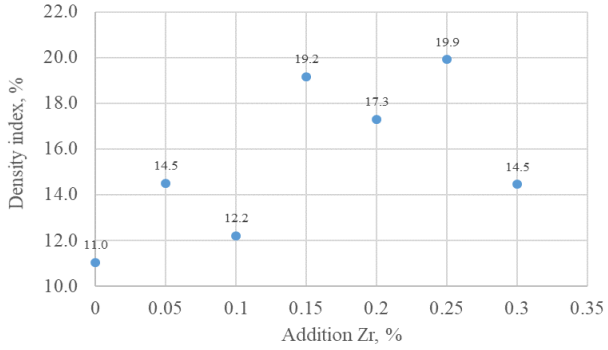

Fig. 4. Dependence of hydrogen solubility on addition of Zr in reference alloy and experimental alloys AlSi9Cu1Mg

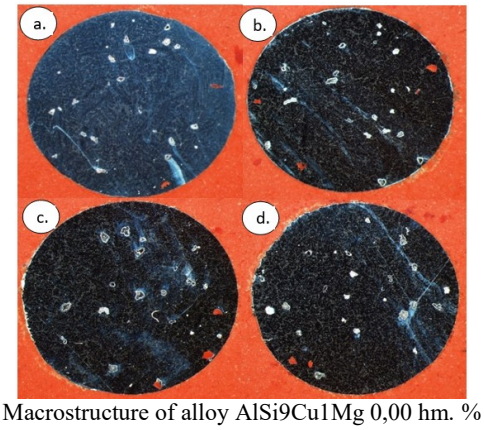

Fig. 5. Macrostructure of alloy AlSi9Cu1Mg 0,00 hm. % Zr (a), 0,10 hm. % Zr (b), 0,20 hm. % Zr (c), 0,25 hm. % Zr (d)

When evaluating the obtained cooling curves of the reference and alloyed variants, it can be stated that the alloyed variants produced a recurrent peak. Green ellipses indicate α phase and eutectic precipitation. The α phase precipitation occurs within a temperature range of 615 to 621 °C. The eutectic is segregated at a temperature of about 561 to 565 °C. Based on the derivative cooling curves (Fig. 6.), it is also possible to observe the elimination of curable phases such as Mg_2Si, at the end of the curve at a temperature of about 550 to 555 °C. Purple ellipses indicate the precipitation of predicted Zr phases in the temperature range 619 to 630 °C. At the given position, the

precipitation of the Zr phases, which was confirmed at a later evaluation of the microstructure, is expected (Fig. 8.). Based on the values obtained, the initial elimination of Zr phases up to subsequent release of α phases or eutectics is assumed for alloyed variants. For experimental alloys with an addition of Zr 0.20 wt. % to 0.30 wt. %, there is a higher degree of supercooling than in experimental alloys with an addition of Zr 0.05 wt. % and 0.10 wt. %. A higher degree of hypothermia represents the precipitation of a large number of larger Zr phases. Also interesting is the change in the precipitation temperatures of the individual phases in the metal matrix of AlSi9Cu1Mg experimental alloys (Table 3.).

Table 3.
Temperature range of excreted basic phases in reference and experimental alloys AlSi9Cu1Mg

Variant, wt. % Zr	0.0	0.05	0.10	0.20	0.25	0.30
α phase, °C	616	618	618	616	620	621
Eutectic Al-Si, °C	565	564	564	561	564	564
Zr phase, °C	-	630	630	623	619	619

By observing the cooling curves (Fig. 6.) of the evaluated experimental alloys, the Zr and α phase elimination change. From Table 3. it can be seen that until the addition of Zr 0.10 wt. %, the α phase and eutectic release temperature were stable. The Zr phase was eliminated at 630 °C when Zr 0.10 wt. % was added. The change occurs when Zr 0.25 wt. % and 0.30 wt. % is added. Exclusion of Zr phases at given contents shifted from 630 °C to 619 °C. In contrast, the α phase is eliminated at 621 °C, which represents an increase of 5 °C over the reference alloy. From the measured values it can be stated that Zr affects the phase formation temperatures in the experimental AlSi9Cu1Mg alloy. Similar conclusions can also be drawn from Hermandez-Sandoval [9]. Here, the eutectic and α phase release temperatures change as the Zr content gradually increases with Ti. [8-9]

2.2. Mechanical Properties and Microstructure

Each experimental variant contained 10 samples (Fig. 2b.) with half of the samples with HT. The arithmetic mean was then determined for each mechanical characteristic and a graph was constructed. The highest tensile strength of R_m without heat treatment of 260 MPa (hereinafter NHT) and 172 MPa after HT was achieved by experimental samples with an addition of Zr 0.25 wt. % (Fig 7a). The best agreed yield strength $Rp_{0.2}$ was achieved for NHT 137 MPa and HT 207 MPa experimental samples with an addition of Zr 0.15 wt. % (Fig. 7a.). When evaluating the elongation A_M (Fig. 8), the best results for NHT 2.0 % and HT 3.2 % were obtained on the reference sample. The modulus of elasticity E in experimental samples NHT has a gradually increasing character up to the value of 0.15 wt. % Zr.

Here, there is a decrease to about 62 and 61 GPa. Its increase is noticeable at the addition of 0.30 wt. % Zr at 66.8 GPa, which is also the highest E value for NHT samples. For HT samples, the highest value of 81.8 GPa was measured at an addition of Zr of 0.20 wt. % (Fig. 7b.). The highest HBW hardness for the NHT category of 71.5 HBW was measured with a Zr 0.15 wt. %, on the other hand, for HT 95.5 HBW in the variant with an addition of Zr 0.05 wt. % (Fig. 7c.). From the obtained mechanical values it is possible to estimate the ability of Zr phases at contents of Zr ≥ 0.10 wt. %, reinforcing the AlSi9Cu1Mg alloy metal matrix. Since the individual melts being prepared were not degassed, there is a higher possibility of influencing the results. For example, there is the variant with the addition of Zr 0.15 wt. % where there is an apparent decrease in R_m. By increasing R_m and E, an AlSi9Cu1Mg alloy is obtained, which is able to withstand the same or higher operating loads even when the functional cross-sections of the casting walls (e.g. cylinder heads) are narrowed.

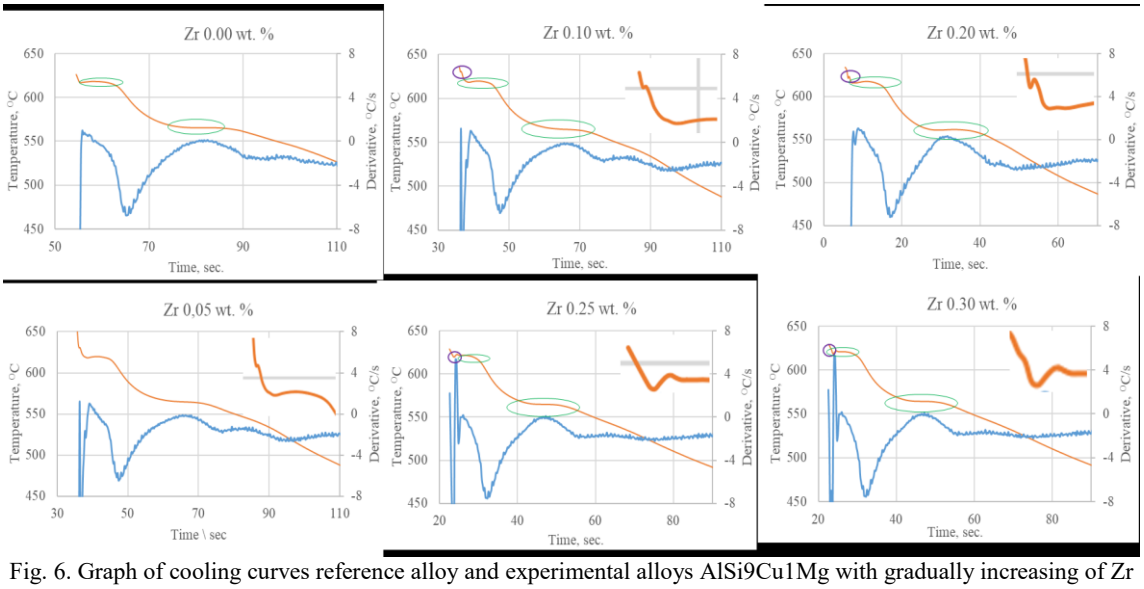

Fig. 6. Graph of cooling curves reference alloy and experimental alloys AlSi9Cu1Mg with gradually increasing of Zr

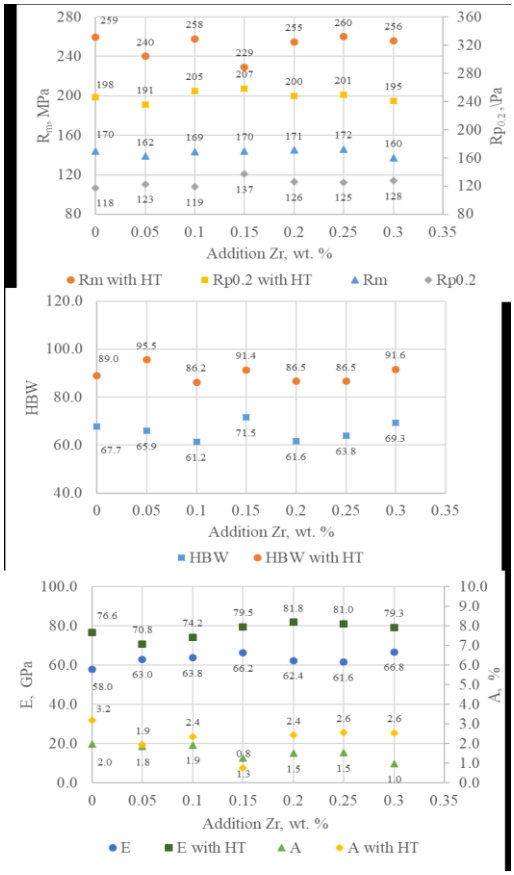

Fig. 7. Dependence of R_m, $Rp_{0,2}$, E, AM and HBW before and after Zr addition

When evaluating the microstructure of AlSi9Cu1Mg experimental alloys with a graded Zr content, the discovery of visible Zr phases already occurs with the addition of Zr 0.10 wt. %. The phases were most often eliminated in the form of needle structures with a smooth surface and split ends (Fig. 8c.). Prior to microstructure image evaluation, samples were etched to ferric phase H_2SO_4 for better resolution and unmistakability of Zr phases. The Zr phases visible on the microstructures are probably intermetallic phases of theAl_3Zr and AlSiZr type. Similar identification is also described in the work of Vončina [1]. As mentioned in Mahmudi's work [4], Zr is characterized by the least diffusion to the α matrix and is therefore preferably eliminated as Al_3Zr. At 500-fold magnification, elimination of Fe phases in the structure and their frequent excretion near Zr phases are observed (Fig. 8c.). After heat treatment, there was a disintegration of large needle phases into small plate-like phases (Fig. 8e., 8f., 8g., 8h.) in experimental variations containing Zr ≥ 0.20 wt. %. When adding Zr 0.20 wt. %, the gradual peeling of smaller portions from the primary secreted Zr phase can be observed (Fig. 8e., 8f.). When observing the microstructures, the most extreme disintegration of the individual needles occurred especially in the variants with the addition of Zr 0.25 wt. % and 0.30 wt. % (Fig. 8g., 8h.). With the addition of Zr 0.15 wt. % and 0.20 wt. %, excluded intermetallic phases in the form of needles in the structure (Fig. 9e., 9f.) are still detectable. After the disintegration of large acicular formations in variants containing Zr ≥ 0.20 wt. % observes a slight increase in R_m and E. The decomposition of large needle-phase phases into smaller plate-like structures, based on the measured results, strengthens the metal matrix of the AlSi9Cu1Mg alloy investigated.

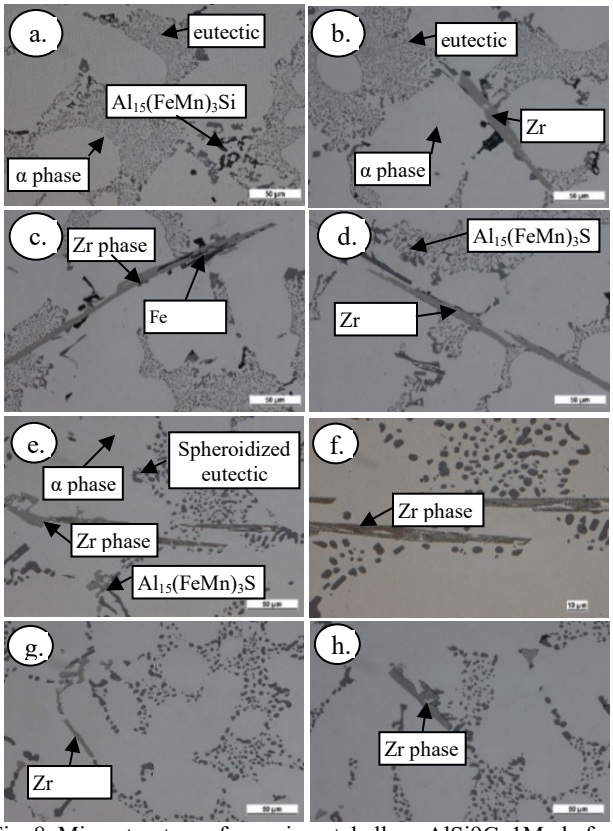

Fig. 8. Microstructure of experimental alloys AlSi9Cu1Mg before heat treated 0,00 wt. % Zr (a), 0,20 wt. % Zr (b), 0,25 wt. % Zr (c), 0,30 wt. % Zr (d), and after heat treated 0,20 wt. % Zr (e), detail 0,20 wt. % Zr (f), 0,25 wt. % Zr (g), 0,30 wt. % Zr (h) etchant H_2SO_4

3. Evaluation

The mechanical properties of R_m and E, in particular, are improved with experimental variations with an addition of Zr 0.20 wt. % and 0.25 wt. %. When comparing the mechanical properties of the experimental samples cast in ceramic moulds with the STN EN 1706 standard for samples cast in sand, significantly higher values were obtained. For R_m and $Rp_{0.2}$ for reference alloys without HT, the improvement over STN EN 1706 is approximately 35 %. After Zr deposition, these values increased by 15 %. Improvement also occurs in A_M, where an increase of up to 90 % occurs. For HBW hardness, the improvement is in the range of 13-20 %. After HT, the mechanical properties of the experimental alloys reached values close to those after casting into metal moulds. A noticeable Zr phase elimination already occurs when Zr 0.10 wt. %. At higher contents of Zr ≥ 0.20 wt. %,

Zr phases are released in the form of large smooth needles intersecting the α phase and the eutectic. Given the excretions, there is an evident increase in R_m, which is attributed to the excreted Zr phases which solidify the metal matrix of the AlSi9Cu1Mg alloy investigated. After the heat treatment, at higher Zr contents, the decomposition of the large needle phases into smaller plate phases is noticeable. The decay increased E by approximately 3 %, compared to the experimental variant with an addition of 0.15 wt. % Zr. (Fig. 9g., 9h.) and of 6 % compared to the reference variant (without Zr addition). By decomposing the Zr phases into smaller plate phases, the metal matrix of the experimental alloy is strengthened based on the measured results.

In experimental samples without HT, the interaction between Fe and Zr phases is noticeable (Fig. 9b., 9c.). Increased growth of skeletal formations was observed in individual structures. These phases were not observed in reference experimental samples. Based on structural analyses, Zr is also expected to act as a corrector in suppressing the negative effect of Fe phases, i.e. it affects the morphology of Fe particles. At the same time, it was observed that Fe phases formed near the Zr phases. It can be stated that by increasing the amount of skeletal formations or clusters of Zr and Fe phases, it affects mechanical properties such as R_m, $Rp_{0.2}$ and E. This is confirmed mainly by increased E values by 4 % at contents of Zr ≥ 0.15 wt. % where the interaction between Fe and Zr phases was recorded. This is expected to increase the fatigue life of the castings. When evaluating the gassing of experimental alloys with hydrogen, a higher gassing rate was found for alloyed variants. For experimental variations with content of Zr> 0.10 wt. %, there was a sharp increase in the DI index (Fig. 4.). The worst results were achieved with the addition of 0.15 wt. % and 0.25 wt. % Zr (Fig. 4.). Zr may increase the gassing rate either in the form of a hydrogen solubility enhancing element in the experimental alloy or above content of Zr ≥ 0.10 wt. % the eliminated Zr phase nuclei trap the excreted hydrogen bubbles. With the addition of Zr 0.05 wt. %, there is a change in the precipitation temperature mainly of α phases in the metal matrix of AlSi9Cu1Mg experimental alloys. This is evident from Table 3. where the precipitation temperature of Zr and α phases was changed mainly at Zr content ≥ 0.20 wt. %. Zr also affects the phase separation process in the metal matrix. [10]

4. Conclusion

The increase in mechanical properties was observed mainly above Zr ≥ 0.15 wt. %. The best mechanical properties were achieved with variants with an addition of Zr 0.20 wt. % and 0.25 wt. %. When evaluating the gassing, the experimental alloys with a higher content of Zr ≥ 0.15 wt. % got a higher DI index. The effect of Zr on the increase of the porosity in castings is assumed. The Zr phases, when evaluating the microstructures (Fig. 9.), form clusters with the Fe phases, eventually causing the transformation of the Fe phases into skeletal formations in the metal matrix. On this basis, it can be stated that Zr act as a corrector in reducing the negative effect of Fe phases in the AlSi9Cu1Mg alloy. The addition of Zr also changes the precipitation temperature of the base phases in the metal matrix. Zr also affects the change in the precipitation temperature, mainly of the α phase. A positive feature is the achievement of mechanical properties after casting into ceramic moulds, which are close to the values of samples cast into metal moulds for and after HT defined by STN EN 1706.

Acknowledgements

The article was created within the project of the grant agency VEGA 1/0494/17. The authors thank the Agency for their support. We would like to thank Alucast s.r.o. and Nemak Slovakia s.r.o. for the technical support of experiments.

Reference

[1] Vončina, M., Medved, J., Kores, S., Xie, P., Cziegler, A. & Schumacher, P. (2018). Effect of molybdenum and zirconium on aluminium casting alloys. *Livarski Vestnik.* 65(1), 36-48.

[2] Medved, J. & Kores, M.V.S. (2018). Development of innovative Al-Si-Mn-Mg alloys with high mechanical properties, *Light Metals 2018. The Minerals, Metals & Materials Society.* 373-380. DOI 10.1007/978-3-319-72284-9_50.

[3] Tsivoilas, D. & Robson, J. D. (2015). Heterogeneous Zr solute segregation and Al3Zr dispersoid distributions in Al-Cu-Li alloys. *Acta Mater.* 93, 73-86. DOI: 10.1016/j.actamat.2015.03.057.

[4] Mahmudi, R., Sepehrband, P. & Ghasemi, H.M., (2006). Improve properties of A319 aluminium casting alloy modified with Zr, *Materials Letters.* 60, 2606-2610. DOI: 10.1016/j.matlet.2006.01.046.

[5] Sepehrband, P., Mahmudi, R. & Khomamizadeh, F., (2004). Effect of Zr addition on the aging behavior of A319 aluminium cast alloy, *Scripta Materialia.* 52, 253-257. DOI: 10.1016/j.scriptamat.2004.10.025.

[6] Bolibruchová, D. Pastirčák, R. (2018). *Foundry metallurgie of non-ferrous metals*. Žilina: EDIS - ŽU UNIZA.

[7] U. N. R. laboratory, (2016). *The Al_3Zr (DO_{23}) structure.* Retrieved February 17, 2016, from http://aflowlib.duke.edu/users/egossett/lattice/struk/d0_23.html.

[8] Kuchař, L., Drápala, J. (2006). *Binary systems of aluminium - mixture and their importance for metallurgy*. Ostrava: VŠB- TU Ostrava.

[9] Hermandez-Sandoval, J., Samuel, A.M. & Vatierra, F.H., (2017). Thermal analysis for detection of Zr-rich phases in Al-Si-Cu-Mg 354-type alloys. *International Journal of Metalcasting.* 11(3), 428-439, DOI: 10.1007/s40962-016-0080-0.

[10] Tillova, E. Chalupova, M. (2009). *Structural analysis of Al-Si alloys.* Žilina: EDIS-ŽU UNIZA.

[11] Pastircak, R., Scury, J., Bruna, M. & Bolibruchova, D. (2017) Effect of technological parameters on the AlSi12 alloy microstructure during crystallization under pressure. *Archives of Foundry Engineering*.17(2), 75-78. ISSN 1897-3310.